ASSESSING DEBRIS-FLOW POTENTIAL BY USING AVIRIS IMAGERY TO MAP SURFACE MATERIALS AND STRATIGRAPHY IN CATARACT CANYON, UTAH

Lawrence Rudd[1] and Erzsébet Merényi[2]

1.0 Introduction

Debris flows are responsible for the loss of hundreds of lives and millions of dollars of property damage each year worldwide (Costa, 1987). As a result of extensive property damage and loss of life there is a pressing need to go beyond just describing the nature and extent of debris flows as they occur. Most of the research into debris-flow initiation has centered on rainfall, slope angle, and existing debris-flow deposits (Costa and Wieczorek, 1987). The factor of source lithology has been recently addressed by studies in the sedimentary terranes of Grand Canyon (Webb et al., 1997; Griffiths et al., 1996) and on the Colorado Plateau as a whole[3]. On the Colorado Plateau shales dominated by kaolinite and illite clays are significantly more likely to be recent producers of debris-flows than are shales in which smectite clays dominate[3].

Establishing the location of shales and colluvial deposits containing kaolinite and illite clays in sedimentary terranes on the Colorado Plateau is essential to predicting where debris flows are likely to occur. AVIRIS imagery has been used to distinguish between types of clay minerals (Chabrillat et al, 2001), providing the basis for surface-materials maps. In the process of producing a model that can be used to estimate the debris-flow hazard in Cataract Canyon, Utah, a map of the stratigraphy and surficial materials found in Cataract Canyon was made from an AVIRIS image taken of this area in 2001. This paper will describe the development of this map, which shows the spectral stratigraphy of the part of Cataract Canyon in and around the area from the mouth of Clearwater Canyon in the south to Gunsight Butte and The Big Ridge in the northwest.

2.0 Debris-Flow Initiation

The mobility and transport competence of debris flows depends on a source of fine-grained material, particularly silt and clay that serves as debris-flow matrix. In Grand Canyon this material is provided by the Hermit Shale, a terrestrial shale containing mostly (95%) illite and kaolinite clays (Griffiths et al, 1996). Kaolinite and illite-rich shales that have been identified as debris-flow source areas on the Colorado Plateau also have relatively high concentrations of exchangeable K^+ and Mg^{++} cations and low amounts (<15%) of Na^+ cations [3]. Smectite clays have the capacity to absorb large amounts of water. One possible mechanism by which smectite clays may reduce the likelihood of debris-flow activity involves rapid absorption of water during initial wetting. Smectites that have absorbed water may swell and seal off underlying areas, effectively stabilizing colluvial deposits by preventing further water absorption.

When a debris flow occurs, sand and smaller-sized particles occupy interstitial spaces in the debris-flow slurry, increasing the density of the matrix and the buoyant forces that contribute to the suspension of larger particles (Beverage and Culbertson, 1964, Hampton, 1975, Rodine and Johnson, 1976). The clay constituents of Grand Canyon debris flows, which provide 2-5 % of the total particles, are 60-80% illite and kaolinite by weight, reflecting the source materials of terrestrial shales and colluvial wedges (Griffiths et al., 1996). Debris flows are responsible for creating virtually all of the rapids in Grand Canyon (Webb et al., 1988). Debris flows that travel significant distances in Grand Canyon occur most often when the Hermit Shale, or its associated colluvial wedges, outcrop at a height of 100 m or more above the river (Griffiths et al., 1996). This association between the Hermit Shale and debris flows in Grand Canyon indicates that lithology is an important factor in identifying debris-flow source areas. Other factors identified by Griffiths et al. (1996) include drainage area, channel gradient, and the aspect of drainages that produce debris flows.

The relationship between the presence of terrestrial shales and an increased probability of debris-flow occurrence that was established in Grand Canyon has been observed in several other canyons on the Colorado Plateau, notably Cataract Canyon and Desolation Canyon in Utah[4]. Debris flows in Cataract Canyon reach the river in one of two ways. First is the occurrence of short-runout debris flows that develop in steep chutes cut into the Honaker Trail Formation and overlying Halgaito Shale and Elephant Canyon Formation. Although these debris-flow chutes are relatively short and generally within the immediate confines of the canyon, they are nonetheless clearly caused by debris-flow activity and are the main source of the debris which is responsible for the formation of

[1] Department of Geosciences, University of Arizona (lrudd@geo.arizona.edu)

[2] Electrical and Computer Engineering Department, Rice University (erzsebet@rice.edu)

[3] Rudd et al (unpublished data) describe debris-flow initiation factors on the Colorado Plateau.

rapids in Cataract Canyon (Fig. 1). The role of debris flows in the creation of rapids in Cataract Canyon has been questioned (Baars, 1987). Direct observation of source regions for the material responsible for the creation of rapids in Cataract Canyon reveal that many of the rapids in Cataract Canyon result from the transportation of debris relatively short distances from canyon walls to the Colorado River. Long runout debris-flows also occur in Cataract Canyon and are responsible for the formation of large debris fans and rapids at the mouths of larger tributaries (Fig. 1), such as Range Canyon and Imperial Canyon.

3.0 Site Description

Ending more than two hundred miles north of the start of Grand Canyon, Cataract Canyon's rapids rival those of Grand Canyon in steepness and intensity (Belknap et al, 1996). Forming the sides of Cataract Canyon are late Paleozoic sedimentary rocks (Fig. 1). Cliffs of interbedded limestone, shale, sandstone, and chert of the Pennsylvanian Honaker Trail Formation are found at river level at the mouth of Clearwater Canyon in the study area and throughout Cataract Canyon (Belknap et al, 1996, Baars, 1987). The Honaker Trail Formation (IPh) is shown in Figure 1 at the mouth of Teapot Canyon. These cliffs are often covered with aprons of colluvium, composed of debris from rocks closer to the canyon rim. Colluvial wedges at the base of the Honaker Trail Formation provide source material for the short-runout debris-flows responsible for creating rapids throughout the Cataract Canyon. These colluvial wedges are clearly shown near the mouth of Teapot Canyon (located slightly upstream of the study area) in Figure 1.

The Permian system in Cataract Canyon starts with the complicated, interfingering Elephant Canyon Formation and Halgaito Shale (Phe). These formations unconformably overlay the Honaker Trail Formation in Canyonlands and are composed of near-shore marine limestones, dolomite, shale and sandstone (Baars, 1987). At Clearwater Canyon these formations are found in cliffs which create Cataract Canyon's inner walls. These cliffs consist of steep limestone walls interspersed with shale slopes (Shown near the mouth of Teapot Canyon in Figure 1). Shale units in both formations contain a high percentage of kaolinite and illite clays (Table 1) and are positioned high enough above the Colorado River to give debris-flows originating at this point sufficient gravitational potential energy to deliver large rapid-forming boulders to the river.

The Cedar Mesa Sandstone (Pc) of Permian age forms the capstone on the walls of Cataract Canyon. Cedar Mesa Sandstone is a generally light-colored, fine to very-fine grained quartz-rich sandstone believed to have been deposited in a near-shore marine environment (Baars, 2000). Outcrops of Cedar Mesa sandstone extend for five or more kilometers northwest and southeast of the Colorado River in the study area, creating an uneven bench of relatively uniform lithology (Fig. 2). To the southeast of Cataract Canyon the Cedar Mesa Sandstone is fractured by northeast–southwest trending normal faults, creating the Grabens Fault Zone. The proximity of Cataract Canyon to a zone of fractured and slumping rocks such as the Grabens Fault Zone is believed to be instrumental in providing much of the rapid-forming debris (Baars, 1987) that has been transported to the river by debris flows. Images of the Cedar Mesa Sandstone (Fig. 2) clearly show the tendency of this formation to form cliffs and uneven tablelands between the Colorado River and the Orange Cliffs. Depressions on the surface of Cedar Mesa Sandstone benches collect water and become potholes that eventually fill with fine windblown slit and clay. Cryptobiotic soil develops in these potholes, stabilizing the windblown sediments. A Pinon–Juniper forest, which is commonly interspersed with large exposures of bare Cedar Mesa Sandstone, has developed on the Cedar Mesa Sandstone benches in Cataract Canyon.

Outside of the inner canyon, the rocks surrounding Cataract Canyon tend to alternate between slope-forming shales and mudstones of terrestrial and near-shore origin and cliff-forming, dominantly eolian sandstones. Immediately above the Cedar Mesa Sandstone is the Organ Rock Shale (Po). This shale is dominated by kaolinite and illite clays (Table 1) and forms a series of slopes in the sixty meters or so of vertical distance between the White Rim sandstone above and the Cedar Mesa Sandstone below. Organ Rock Shale was deposited on low, coastal floodplains (Blakey, 1979) and, in the Cataract Canyon area, tends to be magenta to tan in color, forming unvegetated slopes that trend from northeast to southwest.

The Permian White Rim Sandstone (Pw) is up to 76 m thick in the Cataract Canyon area, dominating the geologic section immediately above the Organ Rock Shale as a cliff-forming, nearly white eolian sandstone (Baars and Molenaar, 1971). On its dip slope the White Rim Sandstone is pox-marked with sediment-filled potholes, areas of cryptobiotic soil, and patches of vegetation.

The Triassic Moenkopi Formation (Trm) lies unconformably above the White Rim Sandstone in Cataract

[4] Webb et al (unpublished data) have studied debris-flow initiation factors in Colorado Plateau bedrock canyons.

Canyon. The surface of the Moenkopi Formation is difficult to characterize. It was formed in a variety of near-shore environments which created up to 150 m of interbedded mudstones, siltstones and sandstones (Baars, 2000). These rocks are strongly interbedded, tending to create a ledgy, uneven surface consisting of both thin layers of sandstones in slopes of reddish-brown mudstone and siltstone and occasional massive sandstone cliffs (Huntoon et al, 1982) (Fig. 2). Vegetation on the Moenkopi slopes varies between dense and sparse, contributing to the non-uniform surface appearance of this formation.

The many members of the Upper Triassic Chinle Formation (Trc) are all continental in origin (Stewart et al, 1972). Surface expression of the Chinle Formation in and around Cataract Canyon is highly varied. The lowermost member of this formation in Canyonlands is the cliff-forming, fluvial sandstone of the Moss Back Member (Fig. 2). Above the Moss Back cliffs the Chinle formation is dominated by slopes of mudstone, shale and siltstone leading up to the base of the massive cliff-forming Wingate Sandstone (Fig. 3) (Baars, 2000). Notable among the members of the Chinle formation is the Petrified Forest Formation which contains significant amount of montmorillonite clay (Table 1). The total thickness of the Chile Formation in the study area is approximately 150 m (Baars, 2000).

The Wingate Sandstone (Jw) forms the highly visible Orange Cliffs on the western edge of the study area. The Wingate is the lowermost Jurassic formation in Canyonlands and is composed of dominantly eolian sandstone deposited by northwest winds (Baars and Molenaar, 1971). Massive cliffs of Wingate Sandstone approximately 100 m high define the edges of the mesas and buttes on the western edge of the study area (Fig. 3). This formation not only forms cliffs; but large blocks of Wingate Sandstone that have fallen from the cliffs are important surface features on the Chinle Formation slope.

Overlying the Wingate Sandstone are the cliffs and shale slopes of the fluvial Kayenta Formation (Jk). The Kayenta Formation is approximately 70 m thick in the study area and forms the topmost cliff-forming unit (Hintze, 1988). Large portions of the mesa and butte tops on the western edge of the study area are exposures of Kayenta Formation. Field observation revealed three different surface expressions for the Kayenta Formation near Cataract Canyon: a shale slope immediately above the Wingate Sandstone, a ledgy sandstone cliff and the tablelands forming the mesa and butte tops.

4.0 Spectra of Surface Materials

AVIRIS data of Cataract Canyon was collected on November 9, 2001 (Fig. 4). This data consists of two approximately northeast-southwest trending flight lines composed of nine individual images. Samples of the major clay-containing surface materials in Cataract Canyon were obtained in May of 2001, November of 2003 and May of 2004. These samples were analyzed at Brown University's RELAB. Figure 5 shows the lab spectra plotted with spectra of montmorillonite, kaolinite, and illite from the U.S. Geological Survey's Spectral Library. An obvious feature on the spectra of the shale, colluvium and debris-flow matrix materials found in Cataract Canyon is the 1.9 µm water absorption band, which matches well in placement and depth with the water absorption band in the illite USGS Spectral Library sample. The characteristic double-absorption feature at 2.2 µm readily visible on the Spectral Library sample of kaolinite is difficult to see in the RELAB samples (Fig. 5).

The materials sampled in Cataract Canyon were dry and very friable. It was not possible to obtain these samples in one piece in order to maintain a surface that would accurately match the ground surface exposed during the AVIRIS flights. All shale, colluvium and debris-flow matrix samples obtained in Cataract Canyon and sent to RELAB were composed of clay, silt, fine sand, and a wide variety of sizes of clay aggregates. Handling and transporting these samples changed the nature of their surfaces considerably, which may also have had an effect on the usefulness of the lab spectra obtained from the samples.

The clay mineralogy of the surface materials samples taken in Cataract Canyon was determined by semi-quantitative x-ray diffraction at the U.S. Geological Survey in Denver, Colorado. The x-ray diffraction data (Table 1) shows that the samples' clay mineralogy is dominated by kaolinite and illite. Only the Honaker Trail Formation and Petrified Forest member of the Chinle Formation samples contain significant amounts of montmorillonite. Figure 5 shows that the sample spectra have some similarities with the spectra of illite and kaolinite at 1.9 and 2.2 µm. There is also a significant dip in the sample spectra between 2.3 and 2.4 µm, a possible indicator of chlorite. The dip in the 2.3 to 2.4 µm region is also shown in the kaolinite and illite spectra.

Debris-flow deposits and colluvium in Cataract Canyon display the double-absorption feature characteristic of kaolinite at 2.2 µm in the AVIRIS spectra. This feature is more pronounced in colluvium than in debris-flow matrix, consistent with the measurements shown in Table 1, and with the observation that the total clay content of

most debris-flows is smaller, and the particle size distribution of debris-flow deposits is even more heterogeneous than that found in a typical colluvial wedge in Cataract Canyon. For clay contents, the debris-flow and colluvium spectra are very similar to each other, a fact that supports the cause and effect link between these two types of surface materials. The failure of colluvial wedges in Cataract Canyon provides the raw material, including clay minerals, necessary for debris-flow initiation.

Spectral features relating to surface material composition are apparent in the class average curves (shown in red on Figure 8). Many of the surface materials shown in Figure 8 are also shown in Figure 5 and in Table 1. AVIRIS spectra, RELAB spectra, and x-ray diffraction data compare favorably for the Honaker Trail Formation and colluvium samples. All three sources of data show the colluvium sampled from Cataract Canyon to have significant kaolinite and illite content. Figure 5 and Figure 8 both show colluvium to have a moderately well-developed kaolinite doublet at 2.2 µm in addition to a small illite absorption band at 2.35 µm. The 1.9 µm water band is poorly developed in the RELAB data for colluvium and better developed in the AVIRIS data. This may be atmospheric effect that would not be present in the RELAB sample and does not necessarily show the presence of significant amounts of smectite. All three sources show the Honaker Trail Formation to contain small amounts of kaolinite and illite and, as shown by a relatively deep 1.9 µm absorption band, montmorillonite.

The AVIRIS spectra of the Moenkopi Formation (Fig. 8) clearly show significant amounts of kaolinite in all but the lower member and relatively low amounts of smectite in all members. This is consistent with the x-ray diffraction data shown in Table 1. All members of the Moenkopi formation also appear to contain illite, although the AVIRIS class-mean spectra do not give a clear indication as to the relative amounts of illite in this formation. In fact the AVIRIS class-mean spectra show illite to be widely present in the study area, which may be of wind-blown origin, especially on sandstone units. Windblown clay deposits, which the AVIRIS image reveals to be widespread in the study area, are also shown on the class-mean graphs to contain at illite and at least some kaolinite.

5.0 Class Map Development

Classification of the AVIRIS image first involved establishing training sites for each of the important surface materials on which this study is focused. Training site selection was based on field reconnaissance of the area. Training sites were chosen both from locations where field spectra were acquired and from notes taken during field trips to the area in 2001, 2003 and 2004.

Selected training sites were analyzed using unsupervised clustering with an advance variant of Self-Organizing Map (SOM) (Kohonen, 1997, DeSieno, 1988). The converged, correctly learned SOM reflects the data structure with fine discrimination among material clusters. Cluster boundaries were extracted with SOM tools in the HyperEye environment (www.ece.rice.edu/HYPEREYE) and the resulting clusters were scrutinized for their correspondence to field notes and the existing 1:62,500 scale geologic map of the area (Huntoon et al, 1982) to obtain a labeling.

With the established labeling, supervised classification was done for the entire AVIRIS image using a hybrid Artificial Neural Network (ANN). The existing SOM formed the middle, hidden layer of the ANN, connected to an output layer that performed supervised learning. The already formed clusters in the SOM middle layer support accurate and sensitive classification. Since this SOM-hybrid architecture handles high-dimensional data vectors without difficulty, prior dimensionality reduction is not needed, allowing finer discrimination of classes with great accuracy. More details on this ANN are given in Merényi et al. (1997), for example.

The final class map produced through this technique isolates 28 classes of surface materials on the AVIRIS image of the study area. Eighteen of these classes represent geologic units present in the image (Fig. 6). Of the remaining ten classes, five show surface materials; gravel (one class), surface clay (one class) and colluvium (three classes). The five remaining surface materials show the Colorado River (one class) and shadows (four classes). The large number of classes shown on the class map clearly shows the diversity of surface materials in the study site.

Outcrops of geologic units and deposits of Quaternary alluvium are shown on the 1:62,500 scale geologic map of the study area (Huntoon et al, 1982). A comparison of this map to the class map (Fig. 7) reveals a strong correlation between the spatial extent of the rock types shown on the geologic map and the equivalent units on the class map. The location of surficial deposits such as Quaternary alluvium also compares well between the two maps. Two nearly parallel normal faults run nearly east-west across the northwest section of the image. Movement along these faults has created an offset in the Chinle, Moenkopi and White Rim Sandstone Formations which is clearly shown on the class map.

A comparison of training sample means to class means was performed to assess classification accuracy. This statistical comparison is shown for fifteen representative study area surface materials in Figure 8. On each graph the training sample means (in blue) and the class means (in red) are seen to overlap very closely throughout virtually the whole spectral curve for each type of surface material. This establishes that the class map is accurately representing the materials that it was trained to show. One standard deviation above and below the training sample mean curve is shown by vertical bars (in blue). All of the class mean curves stay well within the range of one training sample mean standard deviation for all of the surface materials shown which also verifies the good fit between the training sample set and the final class map.

6.0 Conclusions

The occurrence of debris-flow activity in Cataract Canyon is believed to have the same cause as debris-flow activity at Grand Canyon and elsewhere on the Colorado Plateau. In this physiographic province an abundance of clays rich in kaolinite and illite and lacking in smectite, high relief between the Colorado River and a shale-containing unit, and a river-corridor aspect that is aligned with the dominant storm track have been shown to increase the likelihood of debris-flow activity (Griffiths, 1996). With the goal of mapping clay mineralogy and debris-flow potential in Cataract Canyon, an AVIRIS image of this area has been classified using an artificial neural network.

A comparison of the class map to a geologic map of the study area reveals (Fig. 7) that uniform rock outcrops with nearly vertical surfaces are shown most clearly on the classified AVIRIS image. An excellent example of this is the White Rim Sandstone. The distinctive White Rim Sandstone cliff (symbol Pw in Fig. 3) is shown clearly on the classified image in dark green, cutting across the image a little northwest of image center. The offset of geologic units caused by faulting in the study area is also shown clearly by the class map. It is important to point out, however, that the class map is not intended to be a geologic map. It shows surface geology clearly when bare rock surfaces of a single formation dominate in any given pixel. While a geologic map may show a large area being covered by a single formation (such as the Cedar Mesa Sandstone) such a formation shows up as the surface material present on the class map most commonly when it's surface is not dominated by a cover of other, more recent, materials.

The diverse nature of materials on horizontal surfaces is clearly shown on the classified AVIRIS image. Roughly horizontal rock surfaces in the study area are generally heterogeneous, with a mixture of rock, soil, vegetation, and intermittent patches of wind-blown clay in potholes. Wind-blown clay appears throughout the image. The smectite-poor Halgaito Shale Formation shares the same class color as much of the wind-blown clay throughout the image indicating the dominance of kaolinite and illite throughout this area. Kaolinite and illite clays are clearly shown in the image, both in outcrops such as the Organ Rock Shale and in potholes and soil on the dip slopes of sandstone units and in colluvial wedges. Smectites appear in the Honaker Trail Formation and in the Petrified Forest Member of the Chinle Formation. Since Kaolinite and illite clays are widespread it is necessary to look at all of the factors involved in debris-flow formation to locate the areas most likely to produce debris flows.

Class-mean spectra derived from the AVIRIS image agree closely with RELAB lab spectra and x-ray diffraction data for colluvium and the shales in the Honaker Trail Formation, clearly showing the dominance of kaolinite and illite in colluvium and montmorillonite in the Honaker Trail samples. The AVIRIS based class-mean spectra show the widespread presence of illite in the study area and reveal the presence of kaolinite in both surficial deposits such as colluvium and windblown clay and in rock formations believed to be important in debris-flow initiation such as the Organ Rock Shale and Moenkopi Formation.

Further research will investigate the feasibility of using the classified AVIRIS image as a surface materials map in the analysis of debris-flow potential for this area. The AVIRIS based surface materials map will be one layer in a GIS analysis using physical parameters such as relief, aspect, drainage-basin area and height above the Colorado River to assess the debris-flow potential in Cataract Canyon.

7.0 Acknowledgements

Collection and analysis of data used in this study has been supported by the United States Geological Survey (Robert Webb, Project Director), the University of Arizona, and the NASA-funded project "Remote sensing for debris flooding hazard assessment in arid regions" (Vic Baker, Principal Investigator), grant number NAG-9293. Additional thanks to graduate student Mike Mendenhall of Rice University for running the neural classifications in the HYPEREYE environment. HYPEREYE is a project supported by NASA OSSA Applied Information Systems Research Program, NAG-10432.

8.0 References Cited

Baars, D.L., 2000, Geology of Canyonlands National Park, *in* Sprinkel, D.A., Chidsey, T.C. Jr. and Anderson, P.B., eds, Geology of Utah's parks and monuments, Utah Geological Association Publication 28: Salt Lake City, Publishers Press, p. 61-84.

Baars, D.L., 1987, Paleozoic rocks of Canyonlands country, *in* Campbell, J.A., ed., Geology of Cataract Canyon and Vicinity, A Field Symposium-Guidebook of the Four Corners Geological Society, Tenth Field Conference-May 14-17, 199 p.

Baars, D.L. and Molenaar, C.M., 1971, Geology of Canyonlands and Cataract Canyon: Four Corners Geological Society Sixth Field Conference Guidebook, 99 p.

Belknap, B., Belknap, B. and Evans, L.B., 1996, Canyonlands river guide: Denver, Eastwook Printing, 79 p.

Beverage, J.P., and Culbertson, J.K., 1964, Hyperconcentrations of suspended sediment: American Society of Civil Engineers, Journal of the Hydraulics Division, v. 90, p. 117-126.

Blakey, R.C., 1979, Lower Permian stratigraphy of the southern Colorado Plateau *in* Baars, D.L., ed., Permianland: Durango, Four Corners Geological Society, Ninth Field Conference, p. 115-129.

Chabrillat, S., Goetz, A.F., Olsen, H.W. and Krosley, L., 2001, Field and imaging spectrometry for identification and mapping of expansive soils, *in* Van der Meer, F.D.and DeJong, S.M., eds., Imaging spectrometry: Basic principles and prospective applications: Dordrecht, Kluwer Academic Publishers, 403 p.

Clark, R.N., and Roush, T.L., 1984, Reflectance spectroscopy: Quantitative analysis techniques, Journal of Geophysical Research, v.89, p. 6329-6340

Costa, J.E., 1984, Physical geomorphology of debris flows, *in* Costa, J.E. and Fleisher, P.J., eds., Developments and applications of geomorphology: Berlin, Springer-Verlag Publishing, p. 268-317.

Costa, J.E., and Weiczorek, G.F., 1987, Debris flows/avalanches: Process, recognition and mitigation: Geological Society of America, Reviews in Engineering Geology, v. 7, 239 p.

DeSieno, D., 1988, Adding a Conscience to Competitive Learning. Proc. ICNN, New York, July 1988, p. 117-124.

Griffiths, P.G., Webb, R.H., and Melis, T.S., 1996, Initiation and frequency of debris flows in Grand Canyon, Arizona: U.S. Geological Survey Open-File report 96-491.

Hampton, M.A., 1975, Competence of fine-grained debris flows: Journal of Sedimentary Petrology, v. 45, no. 4, p. 834-844.

Hintze, L.F., 1988, Geologic History of Utah: Provo, Brigham Young University, 202 p.

Huntoon, P.W., Billingsley, G.H., and Breed, W.J., 1982, Geologic map of Canyonlands National Park and vicinity: Canyonlands Natural History Association, scale 1:62,500.

Kohonen, T., 1997, Self-Organizing Maps: Springer Series in Information Sciences, 30, Springer, Berlin, Heidelberg, New York, 1995, 1997.

Merényi, E., E.S. Howell, L.A. Lebofsky, A.S. Rivkin (1997) Prediction of Water In Asteroids from Spectral Data Shortward of 3 Microns, *ICARUS* 129, pp 421- 439.

Rodine, J.D., and Johnson, A.M., 1976, The ability of debris, heavily freighted with coarse clastic materials, to flow on gentle slopes: Sedimentology, v. 23, p. 213-234.

Stewart, J.H., Poole, F.G., and Wilson, R.F., 1972, Stratigraphy and origin of the Chinle Formation and related Upper Triassic strata in the Colorado Plateau region: U.S. Geological Survey Professional Paper 690, 336 p.

Webb, R.H., Pringle, P.T., Reneau, S.L., and Rink, G.R., 1988, Monument Creek debris flow, 1984 – Implications for formation of rapids on the Colorado River in Grand Canyon National Park, Arizona: U.S. Geological Survey Professional Paper 1492, 39 p.

Webb, R.H., Melis, T.S., Wise, T.W., and Elliott, J.G., 1996, "The Great Cataract," The effects of late Holocene debris flows on Lava Falls Rapid, Grand Canyon National Park, Arizona: U.S. Geological Survey Open-file Report 96-4.

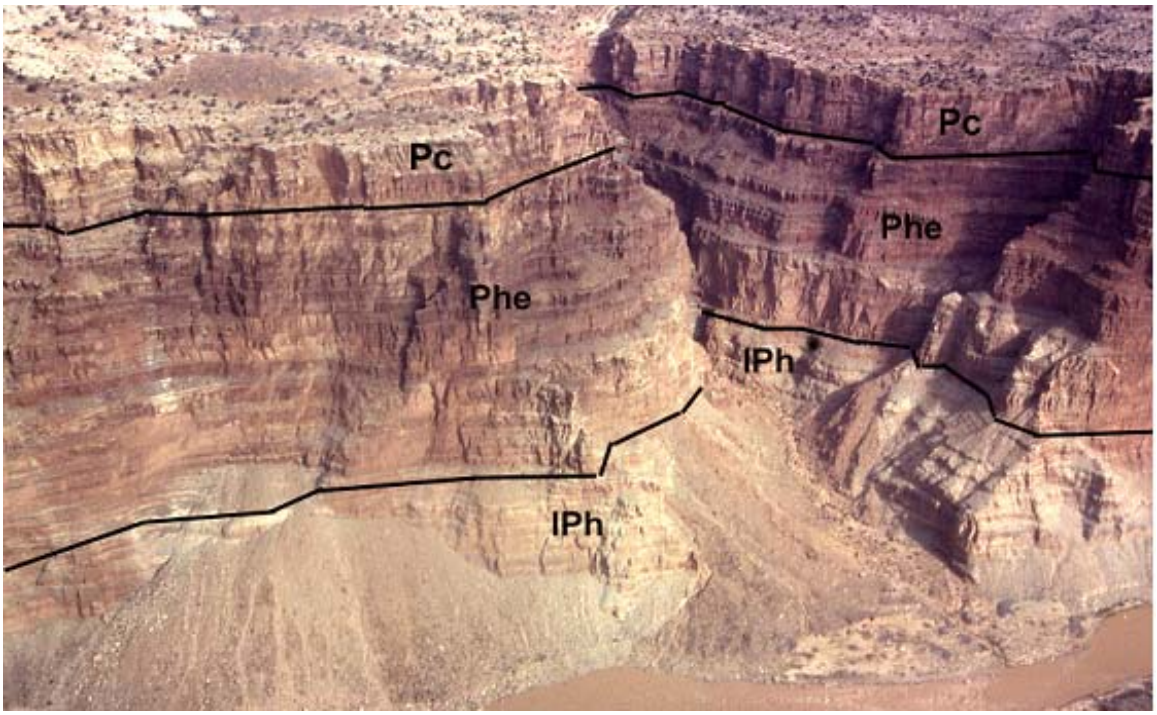

Figure 1. View from the east across the Colorado River toward the mouth of Teapot Canyon with Rapid 22 (Upper Big Drop) in the foreground. The Honaker Trail Formation (IPh) is exposed at river level while the middle half of the inner canyon consists of intertonguing Hailgaito Shale and Elephant Canyon Formation (Phe). Caprock is Cedar Mesa Sandstone (Pc). Note debris fan in Teapot Canyon and colluvial wedges at base of cliff downstream from rapid. (Photo Courtesy of Robert Webb)

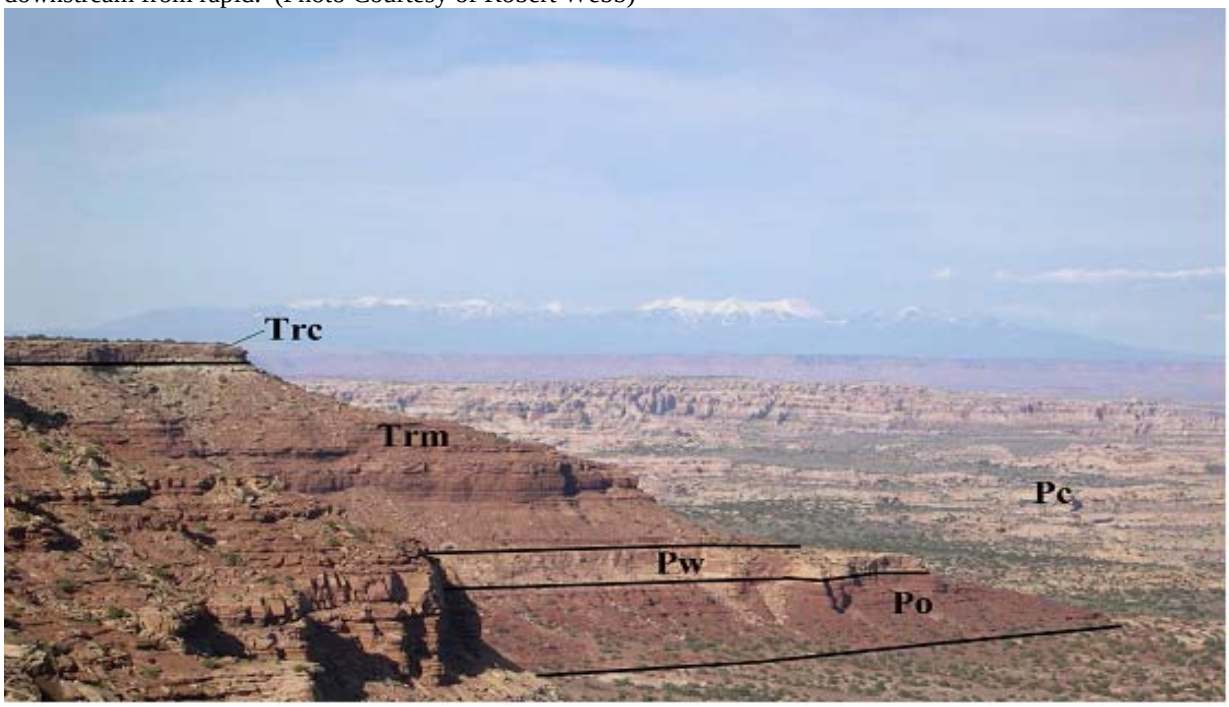

Figure 2. View northeast toward the La Sal Mountains from the headwaters of Teapot Canyon. Cedar Mesa Sandstone (Pc) dominates the foreground and middle ground of the right half of the image. Above the Cedar Mesa Sandstone is the Organ Rock Shale (Po) and White Rim Sandstone. Up section from the White Rim are interbedded sandstones, shales and siltstones of the Moenkopi Formation (Trm). The cap rock of this section is the Moss Back Member of the Chinle Formation (Trc)**.**

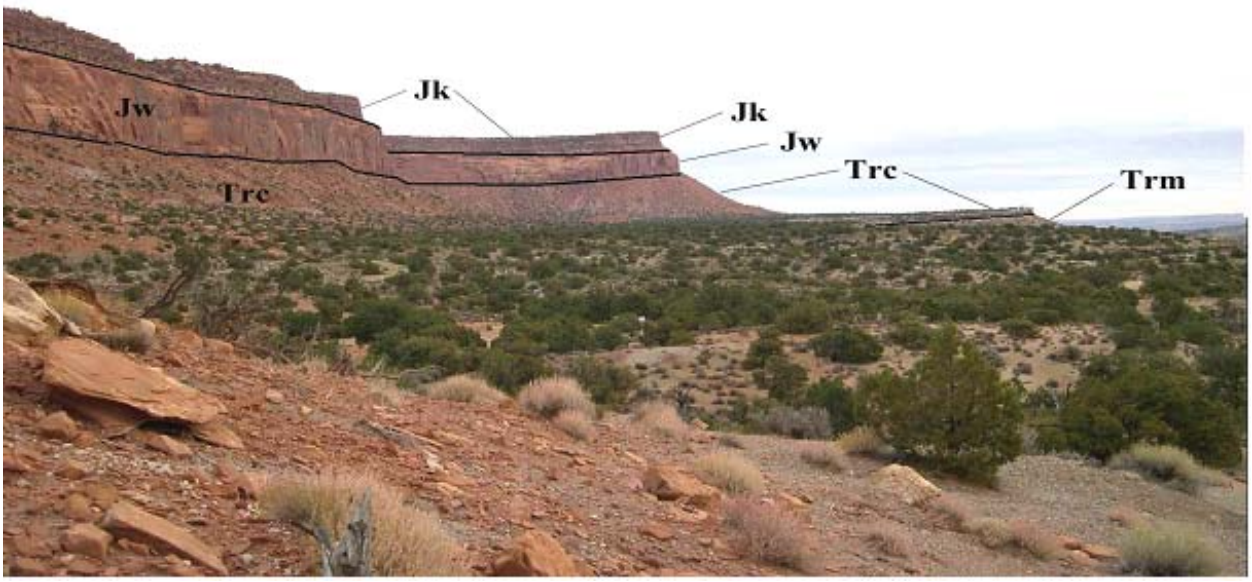

Figure 3. View north to the Orange Cliffs from the area around Sunset Pass. Foreground is dominated by shale slopes of the Chinle Formation (Trc). The point to the right in the distance is the cliff-forming, basal Moss Back Member of the Chinle Formation. Multi-colored Chinle shale slopes ramp up to the base of the massive Wingate sandstone (Jw), forming the Orange Cliffs. The cap rock of the Orange Cliffs is the Kayenta Formation (Jk), which, at this location, consists of a lower, slope-forming unit topped by a cliff-forming sandstone.

Table 1. Semi-quantitative mineralogy by weight percent of clays included in the clay-sized fraction of Cataract Canyon surface material.

Material Sampled	% Illite	% Kaolinite	% Montmorillonite	% Quartz	% Calcite	% Other
Honaker Trail Fm	14	15	55	2	3	11
Elephant Canyon Fm	51	10	0	20	12	7
Halgaito Shale	35	50	0	7	2	6
Organ Rock Fm	38	52	0	2	0	8
Moenkopi Fm						
Lower Member	66	22	0	1	0	1
Upper Member	40	42	3	9	2	4
Chinle Formation						
Petrified Forest Mbr	41	11	42	3	0	3
Sandstone-Mudstone Mbr	32	44	7	7	0	10
Colluvium	24	48	0	6	1	21
Debris-flow matrix	21	30	5	9	16	19

Minerals identified by semi-quantitative x-ray diffraction analysis (Starkey, et al., 1984). Margin of error +/- 20%.

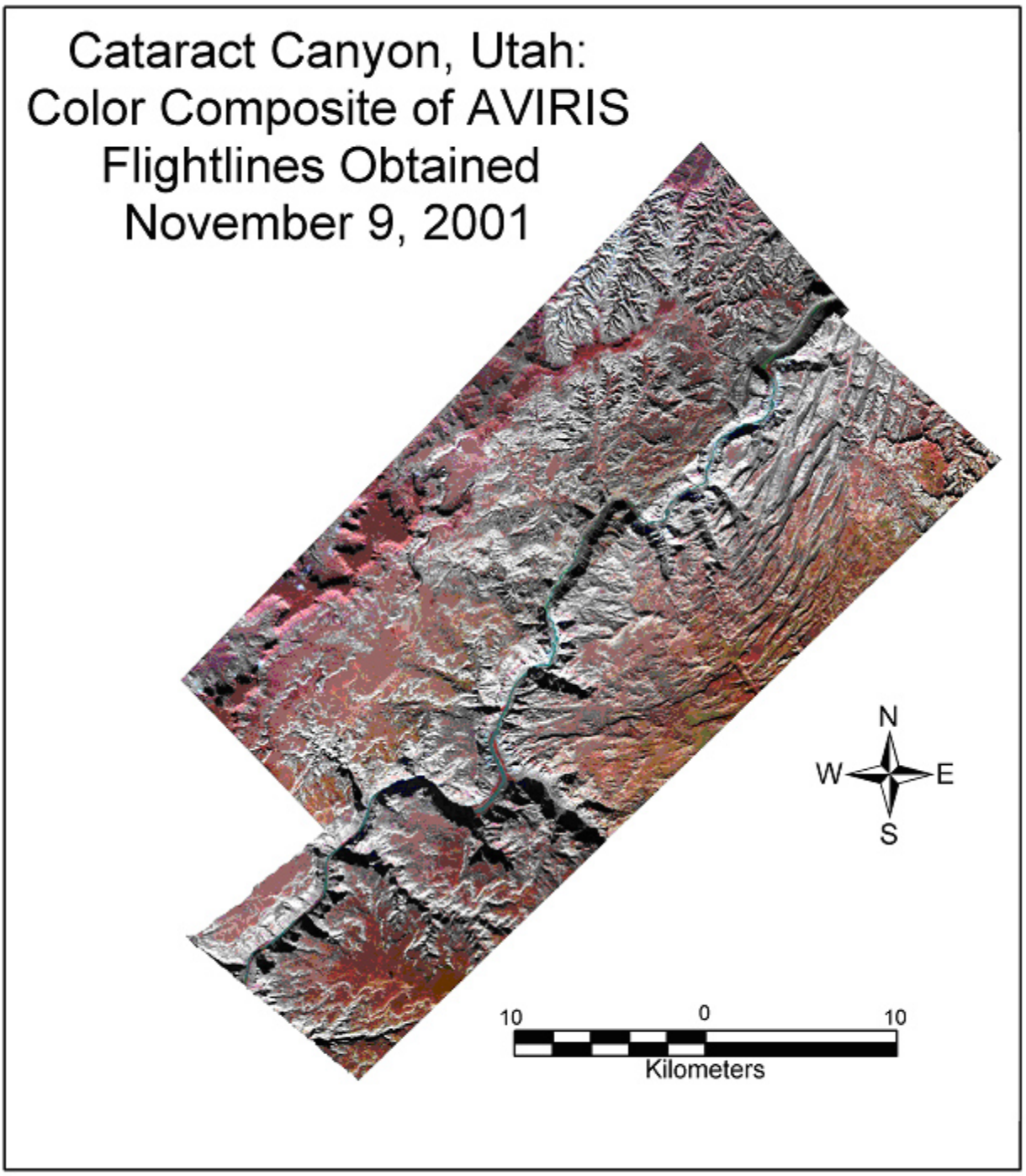

Figure 4. Color composite of the study area flight lines

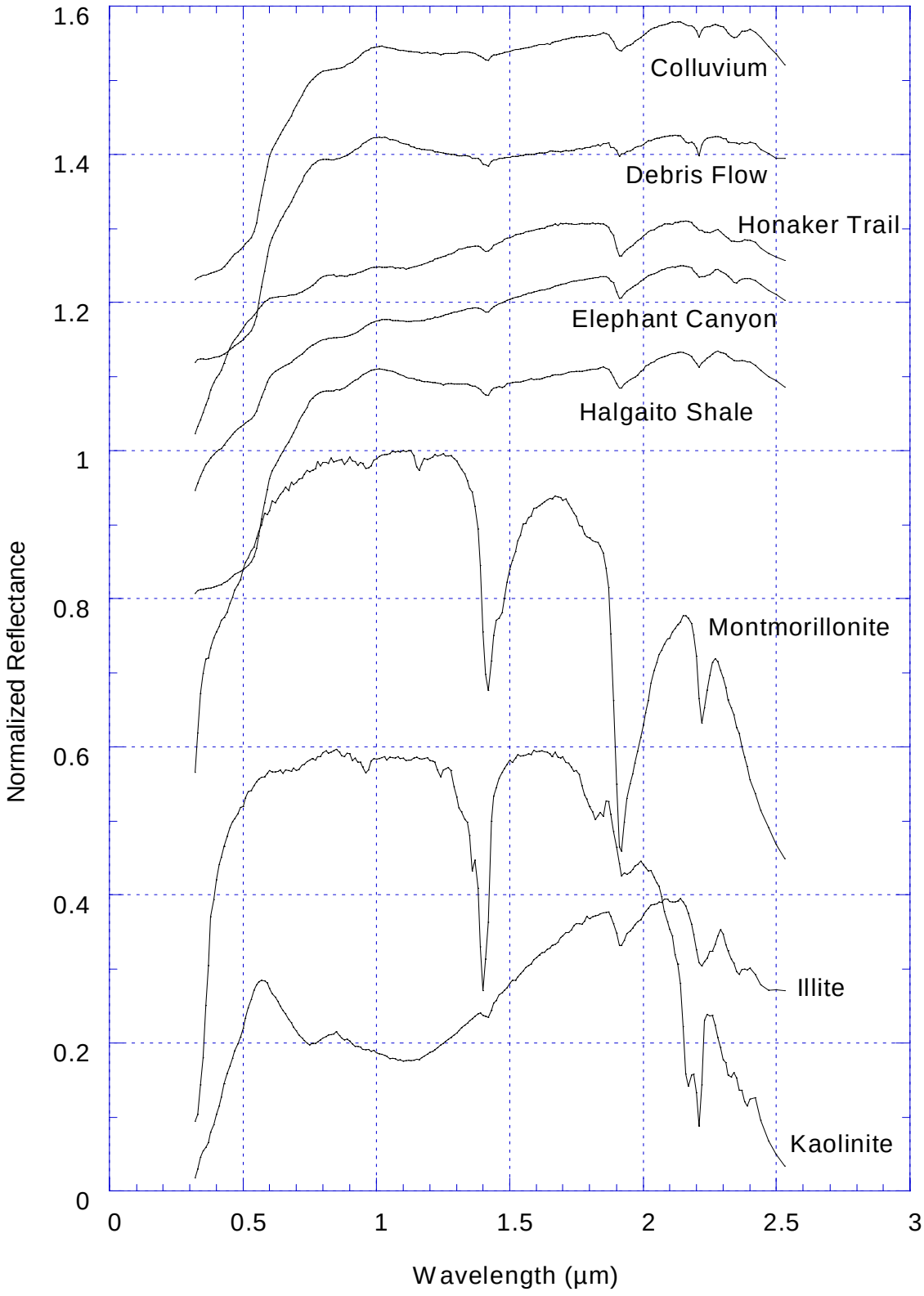

Figure 5. Comparison of Cataract Canyon surface material sample spectra as measured by RELAB and clay mineral spectra from the USGS spectral library. Spectra offset for clarity.

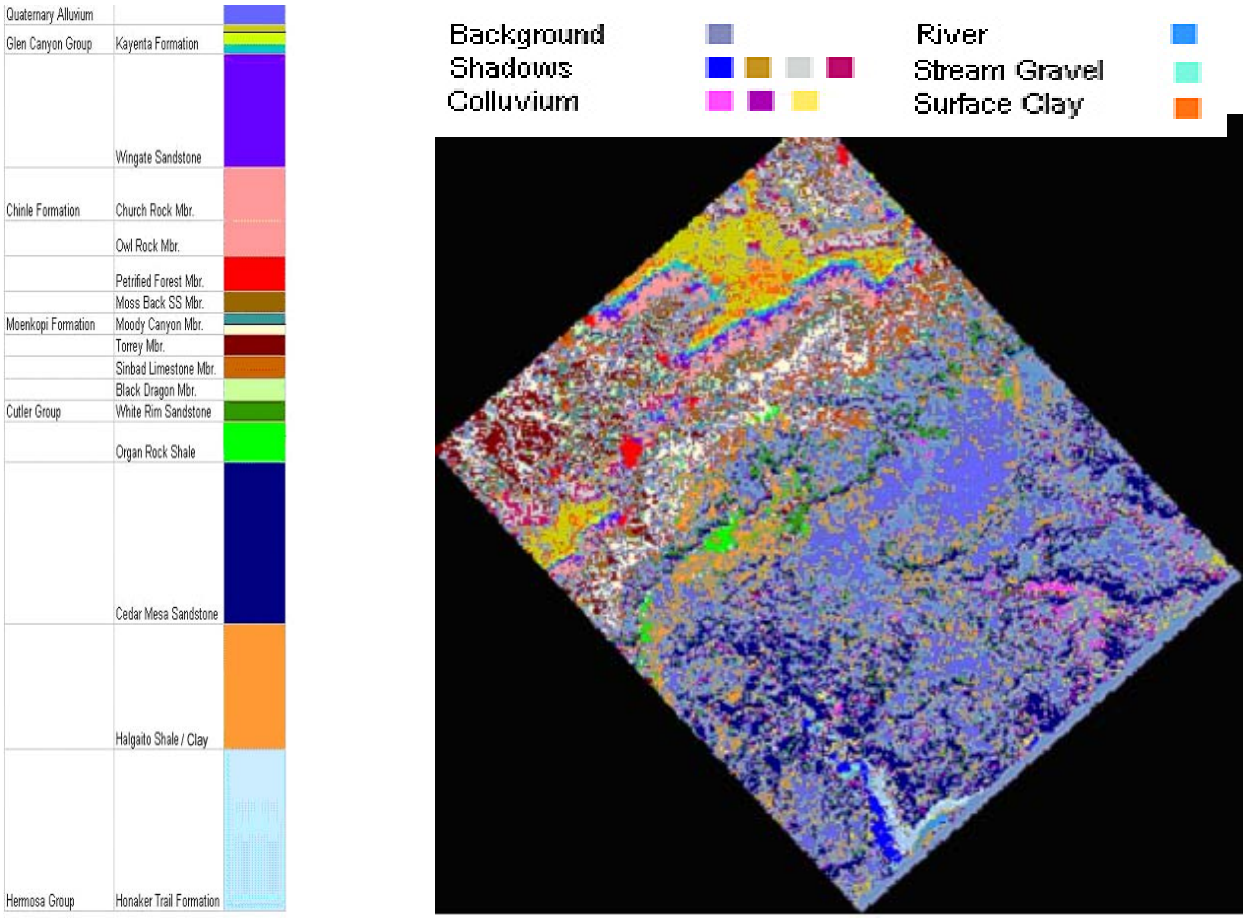

Figure 6. Class map compared to a Stratigraphic section of the study area. Thicknesses of the units shown in the Stratigraphic section are in proportion to each unit's relative thickness in the area surrounding Cataract Canyon. Some formations are shown by more than one color. Surface materials on the class map that are not listed in the Stratigraphic section are shown above the class map. The background color shows pixels that did not fit within any of the 28 classes shown on the image.

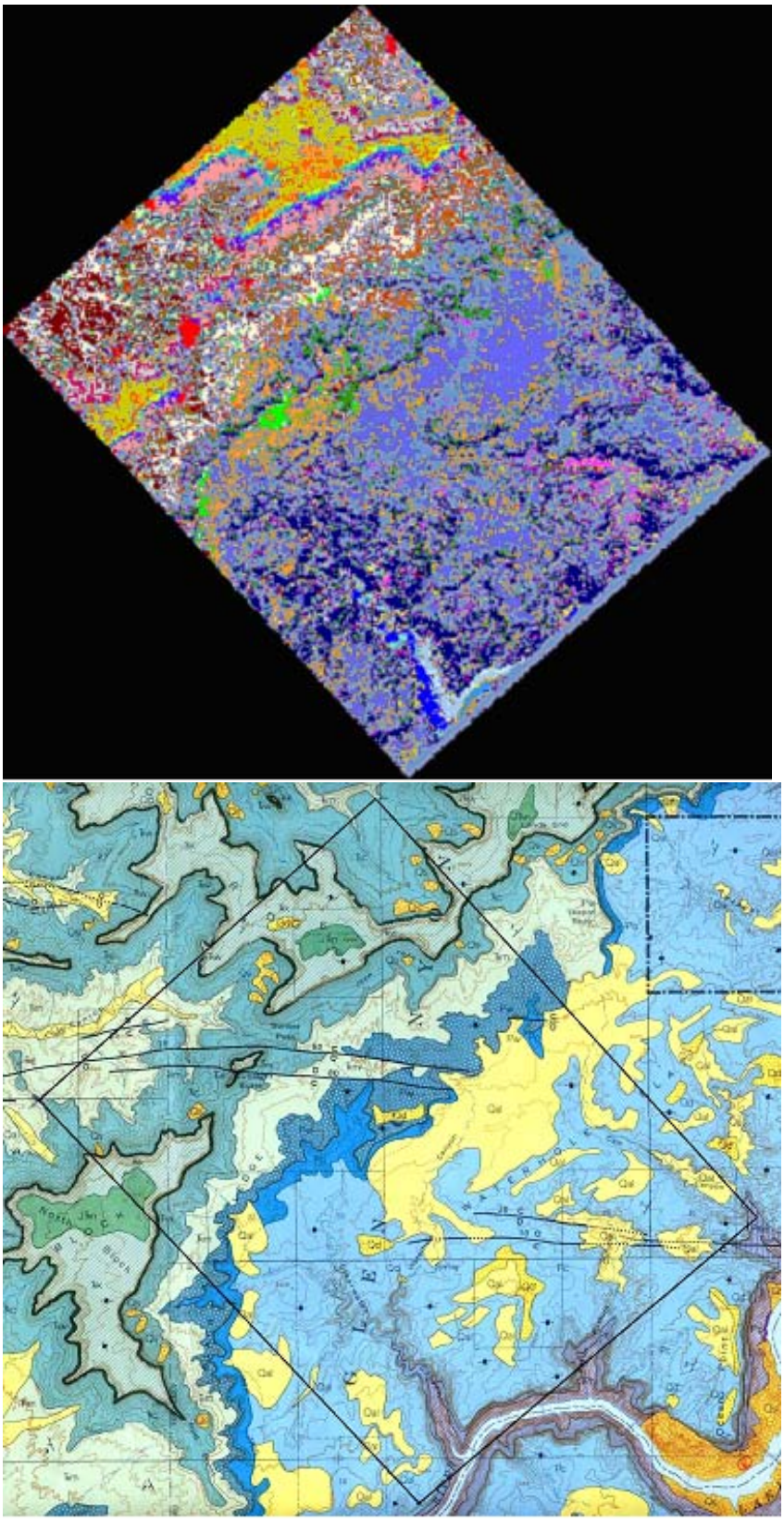

Figure 7. Comparison between the class map and the 1:62500 scale geologic map of the study area (Huntoon et al, 1982). The study area is outlined by a black rectangle on the geologic map.

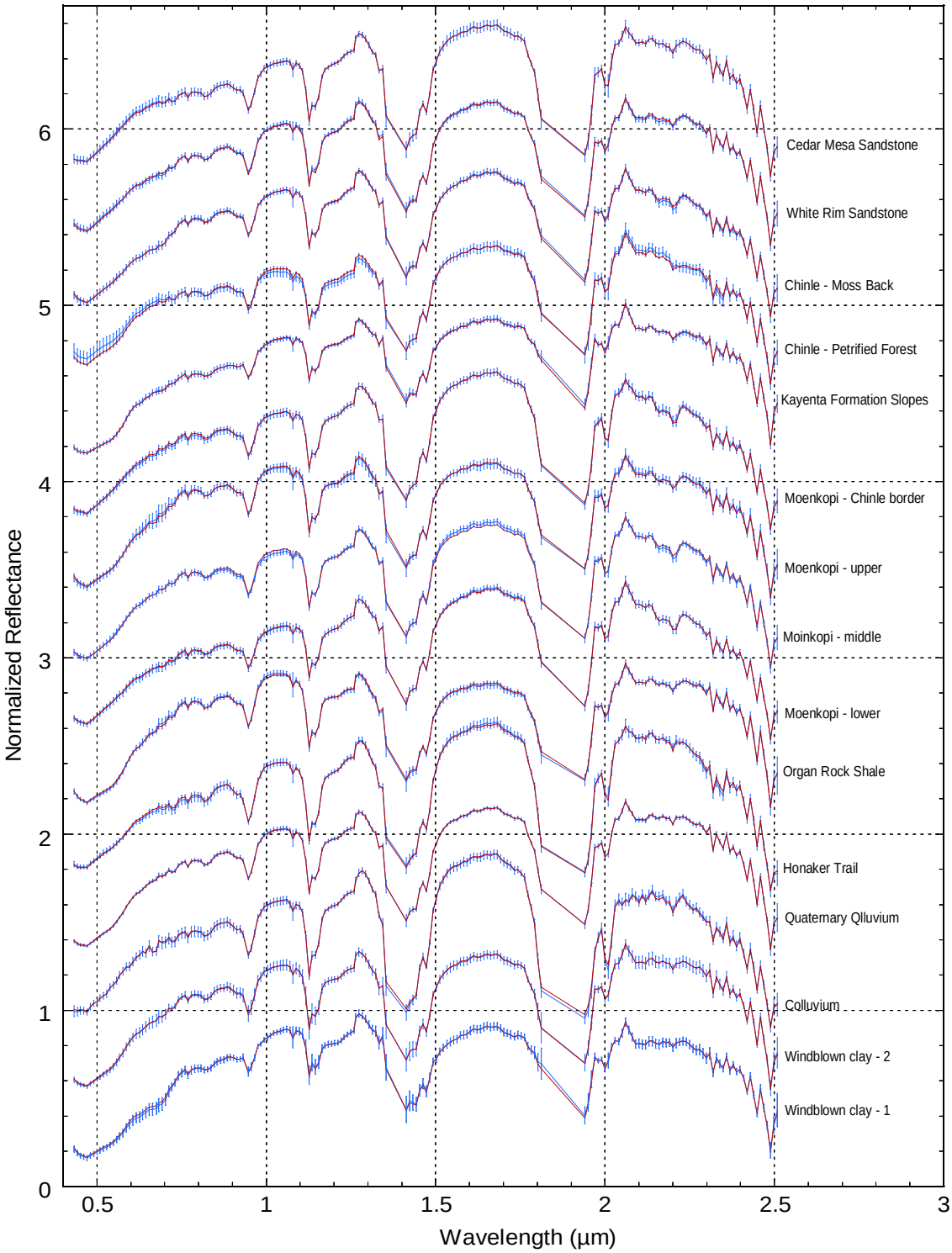

Figure 8. Comparison of training sample means (blue lines) and class means (red lines) for four surface materials in the study area. The blue bars indicate the size of one training sample mean standard deviation. The closeness of fit between class mean and training sample mean curves indicates that the classification is accurate.